VERSITA

Chemical Papers 68 (11) 1555–1560 (2014)
DOI: 10.2478/s11696-014-0613-z

ORIGINAL PAPER

Cu-based atom transfer radical polymerization of methyl methacrylate using a novel tridentate ligand with mixed donor atoms

[a]Fatemeh Saghatchi, [a]Ebrahim Ahmadi*, [b]Zahra Mohamadnia, [a]Hassan Hajifatheali, [a] Hashem Tabebordbar, [a]Farnoosh Karimi

[a]*Department of Chemistry, University of Zanjan, P.O. Box 45195-313, Zanjan, Iran*

[b]*Department of Chemistry, Institute for Advanced Studies in Basic Sciences (IASBS), P.O. Box 45195-159, Gava Zang, Zanjan, Iran*

Received 23 November 2013; Revised 5 May 2014; Accepted 10 May 2014

This study is aimed at atom transfer radical polymerization (ATRP) of methyl methacrylate (MMA) using a novel catalyst. The bis-(2-dodecylsulfanyl-ethyl)-amine (SNS) tridentate ligand with mixed donor atoms was synthesized in high purity using inexpensive reagents and was reacted with copper(I) bromide to produce the CuBr/SNS catalyst. The catalyst mediated living polymerization of MMA yielding polymers with controlled molecular masses and narrow molecular mass distributions (PDI < 1.25). Also, the kinetic plot exhibited a linear increase of $\ln([M]_0/[M])$ versus time, indicating constant concentration of propagating radicals during the polymerization. The products were characterized by ^{1}H NMR, ^{13}C NMR, FT-IR, UV-VIS, GC and elemental analyses (CHNS) and by GPC.

Keywords: atom transfer radical polymerization (ATRP), living polymerization, methyl metacrylate, SNS ligand, catalyst

Introduction

Atom transfer radical polymerization (ATRP) has been a subject of intense research since its discovery by Kato et al. (1995) due to its capability to control polymer design and its general applicability to a wide range of monomers and broad experimental conditions. The fundamental concept of ATRP is the reversible formation of a radical by the transfer of a halogen from an alkyl halide to a transition metal catalyst (Fig. 1). ATRP largely depends on the appropriate equilibrium and dynamics of the reversible formation of a radical; for example the activation (k_{act}) and deactivation (k_{deact}) processes (Fischer, 2001).

One of the main constituents for the determination of the described equilibrium and the dynamics in ATRP is the catalyst prepared from a transition metal and complexing ligands. The study of catalysts has been carried out to develop new ATRP catalysts and understand their catalytic activities using various combinations of transition metals and ligands. Up to now, many transition metals such as Ti (Kabachii et al., 2003), Mo (Le Grognec et al., 2001), Ru (Haas et al., 2006), Ni (Duquesne et al., 2004), Fe (Zhu et al., 2011) and Cu (Sarbu & Matyjaszewski, 2001; Xu et al., 2004; Lee et al., 2005; Pintauer & Matyjaszewski, 2009; Lu et al., 2010) have been successfully used in ATRP of methyl methacrylates (Tang et al., 2006; Cheng et al., 2013), styrenes (Rusen & Mocanu, 2013), acrylates (Datta et al., 2006), acrylonitriles (Chen et al., 2009) and acrylamides (Wever et al., 2012). However, copper is widely used and intensively studied as copper based ATRP catalysts are found superior in terms of activity, adaptability and cost (Tang et al., 2006). Also, different ligands have been employed in copper based systems, including bipyridines (Perrier et al., 2001), terpyridines (Tzanetos et al., 2005), pyridineimines (Goodwin et al., 2004), linear amines (Acar et al., 2006) and branched amines (Tang & Matyjaszewski, 2006). Although ligands with nitrogen

*Corresponding author, e-mail: ahmadi@znu.ac.ir

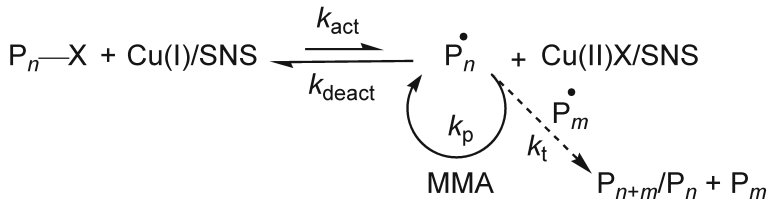

Fig. 1. Proposed mechanism for ATRP with the CuBr/SNS catalyst.

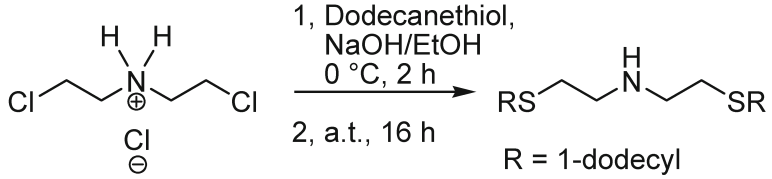

Fig. 2. General method of bis-(2-dodecylsulfanyl-ethyl)-amine (SNS) ligand preparation.

have been extensively studied as ATRP catalysts, copper complexes with sulfur, phosphorous and oxygen ligands or ligands with mixed donor atoms have been comparatively uncharted as ATRP catalyst systems (Cho et al., 2006). Ligands with mixed donor atoms (N and S) can possess higher catalytic activity. Such complexes are interesting because they are sufficiently stable in the presence of acids and therefore can be used to mediate the ATRP of acidic monomers. Polymerization with mixed donors ligands showed both rate enhancement and better control over the molecular masses under similar experimental conditions (Fetzer et al., 2012).

Synthesis of different SNS ligands used in ethylene trimerization has been previously reported (Ahmadi et al., 2011). However, a study on the ATRP of MMA using the novel CuBr/SNS catalyst prepared for the first time is presented here (Fig. 1). In addition, the improvement of the polymerization control by choosing appropriate ligand systems and experimental procedures is demonstrated.

Experimental

All experiments were performed under nitrogen atmosphere in a glovebox or using Schlenk techniques. Ethyl 2-bromoisobutyrate (EBIB, ethyl 2-bromo-2-methylpropanoate), bis(2-chloroethyl)amine hydrochloride, 1-dodecanethiol, tetrahydrofuran (THF), NaOH, acetone, ethanol and methanol were purchased from Merck (Germany) and used as received. CuBr was purchased from Aldrich (USA) and purified according to literature (Matyjaszewski et al., 1997). Methyl methacrylate (MMA) was obtained from Merck (Germany) and distilled over CaH_2 before use. Hexane and diethylether (Merck, Germany) were refluxed over sodium with benzophenone as the indicator and distilled under nitrogen atmosphere prior to use.

^{1}H NMR and ^{13}C NMR spectroscopy were recorded on a Brucker Advance DPX-400 MHZ instruments(Germany) at room temperature in $CDCl_3$ as the solvent and tetramethylsilane (TMS) as the internal standard. FT-IR spectra (in KBr pellet) were obtained on a Shimadzu IR-460 instrument (Kyoto, Japan). UV-VIS spectra were recorded using a Shimadzu UV-1650PC UV-VIS spectrophotometer (Kyoto, Japan). Elemental analysis was performed by a CHNS analyzer system (Elemental, model Vario EL III, Germany). The molecular mass and molecular mass distributions were determined by gel permeation chromatography (GPC) using an Agilent 1100 PS-calibrated with a refractive index detector and a 10^4 Å, 10^3 Å and 500 Å set of PL gel (10 μm) columns (USA). THF was used as the eluent at the flow rate of 1.0 mL min^{-1} at 25 °C. Conversion of the monomer was determined using an Agilent 6890 gas chromatograph (GC) (USA) equipped with a FID detector using an HP-5 column (length of 30 m, i.d. of 0.25 mm, and film thickness of 0.25 μm). The temperature program was set to heating from 50 °C to 140 °C at 30 K min^{-1} and from 140 °C to 300 °C at 40 K min^{-1} under constant pressure with constant inlet and detector temperatures of 310 °C.

Preparation of the bis-(2-dodecylsulfanyl-ethyl)-amine (SNS) ligand

A solution of NaOH (25 mmol) and dodecanethiol (25 mmol) in ethanol (25 mL) was added to a solution of bis(2-chloroethyl)amine hydrochloride (8.33 mmol) in ethanol (16 mL) at 0 °C. The solution was stirred for 2 h at 0 °C and then for another 16 hour at ambient temperature (Fig. 2). Then, it was filtered and evaporated to dryness using a rotary evaporator. The residue was taken up with dry hexane and diethylether, respectively. Finally, the solvent was evaporated under vacuum. Spectral data of the SNS com-

Table 1. Characterization data of prepared compounds

Compound	Appearence	Spectral data
SNS	Colorless oil	IR, $\tilde{\nu}/cm^{-1}$: 720, 736, 885, 1023, 1050, 1120, 1160, 1260, 1376, 1463, 1550–1680, 2850, 2940, 3296 ^{1}H NMR ($CDCl_3$, 400 MHz), δ: 0.86 (6 H, t, CH_3), 1.25–1.31 (36 H, m, $SC_2H_4C_9\mathbf{H}_{18}CH_3$), 1.35 (1H, broad, NH), 1.56 (4H, qn, $SCH_2C\mathbf{H}_2C_{10}H_{21}$), 2.52 (4H, t, $SC\mathbf{H}_2C_{11}H_{23}$), 2.69 (4H, t, $SC\mathbf{H}_2CH_2NH$), 2.86 (4H, t, $SCH_2C\mathbf{H}_2NH$) ^{13}C NMR ($CDCl_3$, 400 MHz), δ: 14.9 (CH_3), 23.5 ($\mathbf{C}H_2CH_3$), 29.3–31.0 ($SC_2H_4\mathbf{C}_7H_{14}C_3H_7$), 32.6–33.1 ($S\mathbf{C}_2H_4C_{10}H_{21}$), 40.0 ($S\mathbf{C}H_2CH_2NH$), 48.9 ($SCH_2\mathbf{C}H_2NH$) UV-VIS, λ_{max}/nm: 215 Elemental analysis: calculated (found), w_i/mass %: C 70.96 (69.35), H 12.55 (12.15), N 2.96 (3.12), S 13.53 (15.56)
CuBr/SNS	Green powder	IR, $\tilde{\nu}/cm^{-1}$: 718, 744, 898, 1023, 1060, 1180, 1190, 1290, 1376, 1463, 1540–1670, 2850, 2940, 3230 ^{1}H NMR ($CDCl_3$, 400 MHz), δ: 0.87 (6 H, CH_3), 1.26 (36 H, $SC_2H_4C_9\mathbf{H}_{18}CH_3$), 1.62 (4H, $SCH_2C\mathbf{H}_2C_{10}H_{21}$), 2.67 (4H, $SC\mathbf{H}_2C_{11}H_{23}$), 3.16 (4H, $SC\mathbf{H}_2CH_2NH$), 4.08 (4H,$SCH_2C\mathbf{H}_2NH$), 9.00–9.30 (1H, broad, NH) ^{13}C NMR ($CDCl_3$, 400 MHz), δ: 14.95 (CH_3), 23.51 ($\mathbf{C}H_2CH_3$), 29.35–31.02 ($SC_2H_4\mathbf{C}_7H_{14}C_3H_7$), 32.65–33.19 ($S\mathbf{C}_2H_4C_{10}H_{21}$), 40.03 ($S\mathbf{C}H_2CH_2NH$), 48.99 ($SCH_2\mathbf{C}H_2NH$) UV-VIS, λ_{max}/nm: 245, 300–450 Elemental analysis: calculated (found), w_i/mass %: C 54.47 (54.39), H 9.63 (9.58), N 2.27 (2.25), S 10.39 (10.44), Cu 10.29 (10.36)
PMMA	White solid	IR, $\tilde{\nu}/cm^{-1}$: 900–960, 1000–1260, 1395–1450, 1700, 3100–2900 ^{1}H NMR ($CDCl_3$, 400 MHz), δ: 0.8–1.3 (CH_3), 1.8–2.1 (CH_2), 3.6 (OCH_3), 3.8 (OCH_2CH_3) ^{13}C NMR ($CDCl_3$, 400 MHz), δ: 16–22 (CH_3), 44–45 (quaternary carbon), 50.81 (CBr), 52 (OCH_3), 51–55 (CH_2), 175–180 (CO)

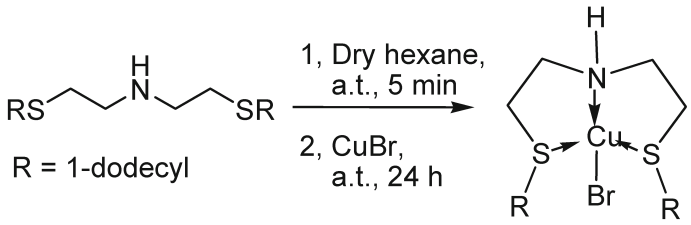

Fig. 3. Preparation of the CuBr/SNS catalyst.

pound are summarized in Table 1.

Preparation of the CuBr/SNS catalyst

The CuBr/SNS catalyst was prepared accorrding to the following method: 0.384 g of SNS (0.81 mmol) was added to 20 mL of dry hexane. The resulting colorless homogeneous solution was stirred at ambient temperature for 5 min under nitrogen atmosphere. Then, 0.116 g of CuBr (0.81 mmol) was added to the reaction flask and the reaction mixture was stirred at ambient temperature for 24 h under nitrogen atmosphere (Fig. 3). The solid product was recovered and washed with 100 mL of diethylether. The light green powder was dried under vacuum at ambient temperature and stored under dry nitrogen in a glovebox. Spectral data of the CuBr/SNS compound are summarized in Table 1.

Polymerization of MMA

A typical polymerization process was run as follows: MMA (20 mL, 188 mmol) was transferred into a deoxygenated Schlenk flask via syringes. After two freeze-pump-thaw cycles, SNS (0.128 g, 0.268 mmol), CuBr (0.039 g, 0.268 mmol) and EBIB (40 μL, 0.255 mmol) were added to the Schlenk flask. After three more freeze-pump-thaw cycles, the Schlenk flask was placed in an oil bath thermostatted at 90 ℃. At given time intervals, 0.90 mL aliquots of the polymerization solution were taken and diluted in THF for GC analysis and filtered through a short alumina column to remove catalyst for the GPC analysis. The conversion of MMA was followed by GC, and molecular masses and molecular mass distributions were determined by GPC. Spectral data of the PMMA compound are summarized in Table 1.

Results and discussion

Ligand and catalyst characterization

FT-IR spectrum of the SNS ligand was compared with that of CuBr/SNS in order to determine the coordination sites involved in chelation. There were some guide peaks in the spectrum of the lignad which were helpful in achieving this goal. Positions of these peaks are expected to change upon chelation. A comparsion showed that the ν(C—N) stretching vibrations in SNS at 1300 cm^{-1} [ν(CS) + ν(CN)], 1260 cm^{-1} and 1120 cm^{-1} were shifted to 1290 cm^{-1}, 1190 cm^{-1} and 1118 cm^{-1} in CuBr/SNS, respectively. Participation of the N—H group in chelation is derived from the shift of the ν(N—$H_{stretch}$) vibration from 3296 cm^{-1} to 3220 cm^{-1} in the spectrum of the catalyst. This band was shifted to lower wave-numbers in the catalyst spectrum, indicating the participation of nitrogen in the coordination of (Cu—N). Other vibrations were not useful since they displayed very weak bands in both the SNS and the CuBr/SNS spectra.

SNS ligands before and after the complexation with copper(I) bromide were compared using UV-VIS. The SNS ligand showed one band at 215 nm that can be attributed to the intramolecular ligand charge transfer (ILCT). CuBr had two broad d–d absorption bands at 230–400 nm and 650–800 nm, indicating a trace amount of Cu(II) due to the oxidation of CuBr.

After the complexation of CuBr with the SNS ligand, the ILCT transition shifted from 215 nm to 245 nm. The metal to ligand charge transfer band (MLCT) (Eisenbach & Schubert, 1993; Shaw et al., 2007) for the CuBr/SNS catalyst appeared between 300–450 nm, which is consistent with the Cu(I) oxidation state. UV spectroscopy confirmed the mononuclear copper(I) complex and the strong coordination between copper and the SNS ligand.

^{1}H NMR spectrum of the SNS ligand was markedly different from that of the CuBr/SNS catalyst. Proton resonance of the SNS ligand was shifted in the catalyst, but the most significant changes occurred for the N—H, $NHCH_2$, SCH_2CH_2NH and $SCH_2C_{11}H_{23}$ signals, which were shifted from 1.35 ppm, 2.86 ppm, 2.69 ppm, 2.52 ppm to 9.15 ppm, 4.08 ppm, 3.16 ppm and 2.67 ppm, respectively. So, the ^{1}H NMR results showed shorter Cu—N interatomic distances than the Cu—S ones because of the bigger anisotropic effect of copper on the chemical shift of $NHCH_2$ than on that of SCH_2CH_2NH. These data are in accordance with the assumptions for the formation of Cu—S and Cu—N bonds. In addition, ^{13}C NMR spectra of SNS and CuBr/SNS showed a very slight chemical shift.

Also, elemental analysis (CHNS) was used to determine the molecular formula of the catalyst. The elemental analysis data suggested the catalyst molecular formula of ML (where M = metal, L = SNS) with the metal to ligand ratio of 1 : 1.

Polymer characterization

FT-IR data of PMMA indicate the details of functional groups present in the synthesized PMMA. A sharp intense peak at 1700 cm^{-1} appeared due to the presence of an ester carbonyl group stretching vibration. The broad peak ranging form 1000–1260 cm^{-1} can be ascribed to the C—O (ester bond) stretching vibration. The broad peak ranging form 3100–2900 cm^{-1} is due to the presence of the C—H aliphatic stretching vibration.

^{1}H NMR spectrum of PMMA showed four signals at δ 0.8–1.3, 1.8–2.1, 3.6 and 3.8, which were related to the α-CH_3, CH_2, OCH_3 and OCH_2CH_3 of the initiator, respectively. Also, mole fractions of rr (syndiotactic), rm (atactic) and mm (isotactic) were calculated. According to the ^{1}H NMR spectral data, syndiotactic, atactic and isotactic percents of PMMA were 57 %, 37.3 % and 5.7 %, respectively. In addition, ^{13}C NMR spectrum was used to assign PMMA. The initiator, monomer units and the end group were identified and the most important recognition was related to the quaternary carbon of the C—Br unit as this showed that the polymerization process is alive. The ^{13}C NMR spectrum showed the C—Br band at δ 50.81.

Polymerization of MMA was carried out by means of CuBr/SNS as the catalyst at 90 °C. The catalyst was fully soluble in the polymerization solution. Solubility of the catalyst in ATRP is significant in polymerization control as the deactivator, here the Cu(II) complex, should be suitably soluble to provide appropriate rate of deactivation (Matyjaszewski et al., 1997). To improve the solubility of the catalyst, the introduction of a long alkyl chain to the ligand has been considered and it led to an improvement of polymerization control, particularly in lowering the molecular mass distribution (PDI) (Matyjaszewski et al., 1997). In our study, the long alkyl chain of SNS increased the activation rate by the electron donating effect, as discussed later, which significantly improved the catalyst solubility. Kinetic data of the MMA polymerization and the dependence of conversion, $\ln([M]_0/[M])$, on time are shown in Fig. 4. The conversion increased smoothly with the increasing reaction time, and conversions higher than 70 % were obtained within about 70 min. The linear relationship between $\ln([M]_0/[M])$ and the reaction time showed that the polymerization follows the first-order kinetic law and the concentration of propagating radicals during the polymerization was nearly constant (Fig. 4). However, since termination occurs continuously, the concentration of the Cu(II) species increases and deviations from linearity can be detected (Matyjaszewski & Xia, 2001).

Fig. 5 and Table 2 show the relationship of molecular mass (M_n), polydispersity index (PDI), monomer conversion and different reaction times. The molecular mass (M_n) of PMMA increased linearly with the monomer conversion, indicating the controlled char-

Table 2. Atom transfer radical polymerization of MMA at 90 °C using CuBr/SNS as the catalyst

Entry	Time	Conversion	M_w	M_n	M_w/M_n
	min	%	Da		–
1	10	53	115020	91449	1.25
2	20	56	122030	101160	1.20
3	30	61	128340	108730	1.18

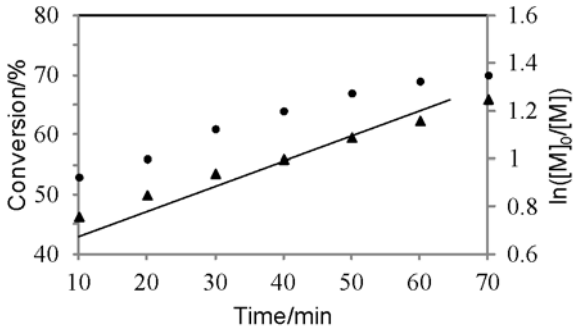

Fig. 4. First-order kinetic plots of MMA using the CuBr/SNS catalyst; monomer conversion (●) and $\ln([M]_0/[M])$ (▲) vs. time.

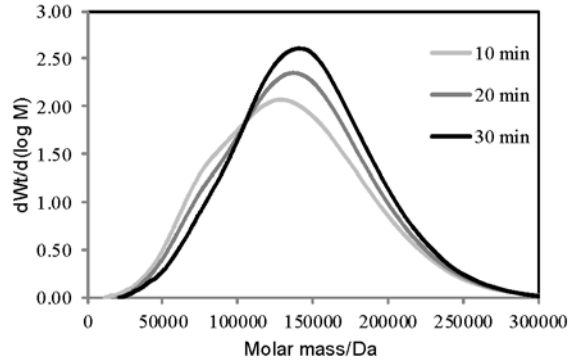

Fig. 5. GPC traces of MMA polymerization using CuBr/SNS as the catalyst at different reaction times.

acter of the polymerization. In addition, the relatively low PDI (< 1.25) and its decrease with the conversion are further proofs of the controlled character of the reaction (Table 2). Thus well-controlled polymerization of MMA with CuBr/SNS was achieved. It is worth to note that the GPC chromatograms in Fig. 5 show considerable tailing in the low molecular region, suggesting continuous termination of the growth of polymeric radicals during the polymerization.

Conclusions

Catalytic activity in copper-mediated ATRP of MMA using SNS, a new tridentate ligand with mixed donor atoms, was studied. Polymerization of MMA with the new catalyst reached high conversion, yielding polymers with controlled molecular mass and low polydispersity (PDI < 1.25). Ligand, catalyst and the obtained polymers were correctly assigned by the NMR, FT-IR, UV-VIS, GC, CHNS analyses as well as by GPC. Overall, this experiment was successfully performed using a novel catalyst based on a copper complex for atom transfer radical polymerization of methyl methacrylate for the first time.

Acknowledgements. The authors gratefully acknowledge the financial support from the INSF organization in Iran.

References

Acar, M. H., Remzi Becer, C., Alper Ondur H., & İnceoğlu, S. (2006). Alkylated linear amine ligands for homogeneous atom transfer radical polymerization. *ACS Symposium Series*, *944*, 98–110. DOI: 10.1021/bk-2006-0944.ch008.

Ahmadi, E., Mohamadnia, Z., & Haghighi, M. N. (2011). High productive ethylene trimerization catalyst based on $CrCl_3$/SNS ligands. *Catalysis Letters*, *141*, 1191–1198. DOI: 10.1007/s10562-011-0594-2.

Chen, H., Yang, L. X., Liang, Y., Hao, Z. H., & Lu, Z. X. (2009). ARGET ATRP of acrylonitrile catalyzed by $FeCl_3$/isophthalic acid in the presence of air. *Journal of Polymer Science Part A: Polymer Chemistry*, *47*, 3202–3207. DOI: 10.1002/pola.23406.

Cheng, C. J., Fu, Q. L., Bai, X. X., Liu, S. J., Shen, L., Fan, W. Q., & Li, H. X. (2013). Facile synthesis of gemini surface-active ATRP initiator and its use in soap-free AGET ATRP mini-emulsion polymerisation. *Chemical Papers*, *67*, 336–341. DOI: 10.2478/s11696-012-0271-y.

Cho, H. Y., Han, B. H., Kim, I., & Paik, H. J. (2006). New tridentate ligands with mixed donor atoms for Cu-based atom transfer radical polymerization. *Macromolecular Research*, *14*, 539–544. DOI: 10.1007/bf03218721.

Datta, H., Bhowmick, A. K., & Singha, N. K. (2006). Atom transfer radical polymerization (ATRP) of ethyl acrylate: Its mechanistic studies. *Macromolecular Symposia*, *240*, 245–251. DOI: 10.1002/masy.200650830.

Duquesne, E., Degée, P., Habimanab, J., & Dubois, P. (2004). Supported nickel bromide catalyst for atom transfer radical polymerization (ATRP) of methyl methacrylate. *Chemical Communications*, *6*, 640–641. DOI: 10.1039/b316645g.

Eisenbach, C. D., & Schubert, U. S. (1993). Synthesis and chain extension of bipyridine-terminated polyethers with copper(I) ions. *Macromolecules*, *26*, 7372–7374. DOI: 10.1021/ma00078a041.

Fetzer, L., Toniazzo, V., Ruch, D., & di Lena, F. (2012). Transition-metal catalysts for controlled radical polymerization: A first update. *Israel Journal of Chemistry*, *52*, 221–229. DOI: 10.1002/ijch.201100117.

Fischer, H. (2001). The persistent radical effect: A principle for selective radical reactions and living radical polymerizations. *Chemical Reviews*, *101*, 3581–3610. DOI: 10.1021/cr990124y.

Goodwin, J. M., Olmstead, M. M., & Patten, T. E. (2004). Identification and characterization of monoanionic tripodal tetradentate ligand complexes of copper(I) and copper(II) involved in halogen atom transfer reactions. *Journal of the American Chemical Society*, *126*, 14352–14353. DOI: 10.1021/ja045003g.

Haas, M., Solari, E., Nguyen, Q. T., Gautier, S., Scopelliti, R., & Severin, K. (2006). A bimetallic ruthenium complex as a catalyst precursor for the atom transfer radical polymerization of methacrylates at ambient temperature. *Advanced Synthesis & Catalysis*, *348*, 439–442. DOI: 10.1002/adsc.200505318.

Kabachii, Y. A., Kochev, S. Y., Bronstein, L. M., Blagodatskikh, I. B., & Valetsky, P. M. (2003). Atom transfer radical polymerization with Ti(III) halides and alkoxides. *Polymer Bulletin*, *50*, 271–278. DOI: 10.1007/s00289-003-0157-9.

Kato, M., Kamigaito, M., Sawamoto, M., & Higashimura, T. (1995). Polymerization of methyl methacrylate with the carbon tetrachloride/dichlorotris-(triphenylphosphine)ruthenium(II)/methylaluminum bis(2,6-di-*tert*-butylphenoxide) initiating system: Possibility of living radical polymerization. *Macromolecules*, *28*, 1721–1723. DOI: 10.1021/ma00109a056.

Le Grognec, E., Claverie, J., & Poli, R. (2001). Radical polymerization of styrene controlled by half-sandwich Mo(III)/Mo(IV) couples: All basic mechanisms are possible. *Journal of the American Chemical Society*, *123*, 9513–9524. DOI: 10.1021/ja010998d.

Lee, Y. W., Kang, S. M., Yoon, K. R., Chi, Y. S., Choi, I. S., Hong, S. P., Yu, B. C., Paik, H. J., & Yun, W. S. (2005). Formation of carbon nanotube/glucose-carrying polymer hybrids by surface-initiated, atom transfer radical polymerization. *Macromolecular Research*, *13*, 356–361. DOI: 10.1007/bf03218466.

Lu, G., Lib, Y. M., Lu, C. H., Xu, Z. Z., & Zhang, H. (2010). AGET ATRP of methyl methacrylate by silica-gel-supported copper(II) chloride/2-(8-heptadecenyl)-4,5-dihydro-1*H*-imidazole-1-ethylamine. *Designed Monomers & Polymers*, *13*, 509–522. DOI: 10.1163/138577210x530585.

Matyjaszewski, K., Patten, T. E., & Xia, J. H. (1997). Controlled/"living" radical polymerization. Kinetics of the homogeneous atom transfer radical polymerization of styrene. *Journal of the American Chemical Society*, *119*, 674–680. DOI: 10.1021/ja963361g.

Matyjaszewski, K., & Xia, J. H. (2001). Atom transfer radical polymerization. *Chemical Reviews*, *101*, 2921–2990. DOI: 10.1021/cr940534g.

Perrier, S., Armes, S. P., Wang, X. S., Malet, F., & Haddleton, D. M. (2001). Copper(I)-mediated radical polymerization of methacrylates in aqueous solution. *Journal of Polymer Science Part A: Polymer Chemistry*, *39*, 1696–1707. DOI: 10.1002/pola.1147.

Pintauer, T., & Matyjaszewski, K. (2009). Structural and mechanistic aspects of copper catalyzed atom transfer radical polymerization. *Topics in Organometallic Chemistry*, *26*, 221–251. DOI: 10.1007/978-3-540-87751-6_7.

Rusen, E., & Mocanu, A. (2013). Atom transfer radical emulsion polymerization (emulsion ATRP) of styrene with water-soluble initiator. *Colloid and Polymer Science*, *291*, 2253–2257. DOI: 10.1007/s00396-013-2955-4.

Sarbu, T., & Matyjaszewski, K. (2001). ATRP of methyl methacrylate in the presence of ionic liquids with ferrous and cuprous anions. *Macromolecular Chemistry and Physics*, *202*, 3379–3391. DOI: 10.1002/1521-3935(20011101)202:17<3379::aid-macp3379>3.0.co;2-3.

Shaw, G. B., Grant, C. D., Shirota, H., Castner, E. W., Meyer, G. J., & Chen, L. X. (2007). Ultrafast structural rearrangements in the MLCT excited state for copper(I) bisphenanthrolines in solution. *Journal of the American Chemical Society*, *129*, 2147–2160. DOI: 10.1021/ja067271f.

Tang, W., & Matyjaszewski, K. (2006). Effect of ligand structure on activation rate constants in ATRP. *Macromolecules*, *39*, 4953–4959. DOI: 10.1021/ma0609634.

Tang, H. D., Arulsamy, N., Radosz, M., Shen, Y. Q., Tsarevsky, N. V., Braunecker, W. A., Tang, W., & Matyjaszewski, K. (2006). Highly active copper-based catalyst for atom transfer radical polymerization. *Journal of the American Chemical Society*, *128*, 16277–16285. DOI: 10.1021/ja0653369.

Tzanetos, N. P., Andreopoulou, A. K., & Kallitsis, J. K. (2005). Side-chain terpyridine polymers through atom transfer radical polymerization and their ruthenium complexes. *Journal of Polymer Science Part A: Polymer Chemistry*, *43*, 4838–4848. DOI: 10.1002/pola.20950.

Wever, D. A. Z., Raffa, P., Picchioni, F., & Broekhuis, A. A. (2012). Acrylamide homopolymers and acrylamide–*N*-isopropylacrylamide block copolymers by atomic transfer radical polymerization in water. *Macromolecules*, *45*, 4040–4045. DOI: 10.1021/ma3006125.

Xu, W. J., Zhu, X. L., Cheng, Z. P., Chen, J. Y., & Lu, J. M. (2004). Atom transfer radical polymerization of hexadecyl acrylate using CuSCN as the catalyst. *Macromolecular Research*, *12*, 32–37. DOI: 10.1007/bf03218992.

Zhu, G. H., Zhang, L. F., Zhang, Z. B., Zhu, J., Tu, Y. F., Cheng, Z. P., & Zhu, X. L. (2011). Iron-mediated ICAR ATRP of methyl methacrylate. *Macromolecules*, *44*, 3233–3239. DOI: 10.1021/ma102958y.